



Published in final edited form as:

*Bioconjug Chem.* 2009 February ; 20(2): 205–208. doi:10.1021/bc8004182.

## Self-Assembling DNA Quadruplex Conjugated to MRI Contrast Agents

Jianfeng Cai<sup>†</sup>, Erik M. Shapiro<sup>\*,‡</sup>, and Andrew D. Hamilton<sup>\*,†</sup>

<sup>†</sup>*Department of Chemistry, Yale University, 225 Prospect Street, New Haven, CT 06511*

<sup>‡</sup>*Department of Diagnostic Radiology, Yale University School of Medicine, 300 Cedar Street, New Haven, CT 06520*

### Abstract

We report the preparation and magnetic resonance (MR) characterization of new MRI contrast agents based on gadolinium complexes conjugated to a self-assembling DNA quadruplex scaffold. As a single gadolinium-DOTA chelated DNA strand, the  $r_1$  molar relaxivity is  $6.4 \text{ mM}^{-1} \text{ s}^{-1}$  per Gd and increases to  $11.7 \text{ mM}^{-1} \text{ s}^{-1}$  per Gd upon formation of a DNA quadruplex. Similar results were obtained when a gadolinium-DOTA dendrimer was conjugated to DNA, the  $r_1$  molar relaxivity increasing to  $12.9 \text{ mM}^{-1} \text{ s}^{-1}$  per Gd upon the formation of DNA quadruplex, compared to that of  $6.0 \text{ mM}^{-1} \text{ s}^{-1}$  for single strand of gadolinium-DOTA dendrimer chelate. This yields an  $r_1$  molar relaxivity of 154.8 and  $46.8 \text{ mM}^{-1} \text{ s}^{-1}$  per DNA quadruplex molecular complex based on DOTA dendrimer or monomer, respectively. Importantly, the DNA quadruplex scaffold of the contrast agent is approximately  $2.5 \text{ nm}^3$  in size, potentially enabling this type of contrast agent to be used for targeted delivery in vivo to detect specific cells or tissues, even behind intact blood vessels.

The targeted and non-invasive detection of specific pathologies in humans is a major research focus in the broad area of bioimaging sciences. To this end, magnetic resonance imaging (MRI) has emerged as an important and useful imaging strategy. As a noninvasive imaging technique, MRI provides three dimensional images of anatomic structures of living organisms at high spatial resolution ( $\sim 100$  microns isotropic) in scan times of less than 30 minutes (1). Similar to other molecular imaging technologies, targeted MRI requires the delivery of specific probes to detect underlying biological abnormalities. Commonly used MR targeting constructs include paramagnetic liposomes (2), paramagnetic perfluorocarbon nanoparticles (3), superparamagnetic iron oxide nanoparticles (4) and small paramagnetic chelates (5). Almost always, the paramagnetic metal used is  $\text{Gd}^{3+}$  because of its ability to increase the longitudinal relaxation rate ( $R_1$ ) of water protons and therefore to enhance the observable signal. Superparamagnetic iron oxide nanoparticles create local magnetic field distortions which increases the transverse relaxation rate ( $R_2$ ), effectively destroying signal and making dark contrast in images.

Targeted MRI has had a major impact on the detection and treatment of cancer (6) and atherosclerosis (7). This is largely due to the accessibility of blood vessels in these diseases, as most nanoparticle formulations are on the order of 30 to  $>100 \text{ nm}$  in diameter, and are too

<sup>a</sup>By assuming an average distance of  $3.4 \text{ \AA}$  between base-pairs, and a distance of  $11 \text{ \AA}$  between adjacent guanines in each tetrad, the volume of DNA quadruplex scaffold was calculated to be  $1.1 \times 1.1 \times 2.0 = 2.5 \text{ nm}^3$ .

andrew.hamilton@yale.edu and erik.shapiro@yale.edu.

Supporting information available: Procedures on oligonucleotides synthesis, quadruplex formation, Gd(III) ion incorporation and measurements of the relaxivities of 1X, 2X, 1Y and 2Y. This information is available free of charge via the Internet at <http://pubs.acs.org>.

large to extravagate from undamaged blood vessels (8). Furthermore, even if they were to escape into the extracellular space, their large size limits their diffusion within the tissue (9). Diseases, such as small, non-aggressive tumors, Alzheimer's plaques and ischemic tissues, which manifest themselves without leaky blood vessels or behind the intact blood brain barrier have been challenging to target. Thus, the large size of most nanoparticle constructs limits their general usage, and there is much interest in synthesizing ultrasmall nanoparticles for targeted MRI (10).

A significant barrier to the development of new generations of small Gd based MR agents is the low molar relaxivity ( $r_1$ ) of chelated gadolinium. Clinical contrast agents have molar  $r_1$  of 3-7  $\text{mM}^{-1} \text{s}^{-1}$  (8), resulting in the need for high concentrations to enhance the MRI signal (11). Significant research has focused on increasing the rotational correlation time ( $\tau_R$ ) of the gadolinium containing complex to increase molar relaxivity and hence, to obtain more efficient contrast agents (12). For example, clinically used small-molecule contrast agents have been conjugated to high-molecular-weight macromolecules including proteins (11), polymers (13), and self-assembled peptide amphiphile nanofibers (14). This has resulted in increases of  $r_1$  to 7.3, 19.3, and 22.8  $\text{mM}^{-1} \text{s}^{-1}$ , respectively. Recently, several contrast agents with even higher relaxivities have been reported. For example, Aime et al. showed that a lipophilic Gd-AAZTA complex bound to albumin had a relaxivity of 84  $\text{mM}^{-1} \text{s}^{-1}$  (15). Yang et al. also designed protein-based contrast agents and demonstrated relaxivities of 35-130  $\text{mM}^{-1} \text{s}^{-1}$  (16). Caravan et al. reported dual binding GdDTPA tetramers that showed relaxivities of 46-50.8  $\text{mM}^{-1} \text{s}^{-1}$  when bound to albumin (17). Wilson et al. prepared gadolinium-carbon nanotube complexes with relaxivities of 159-179  $\text{mM}^{-1} \text{s}^{-1}$  (18). However, MRI contrast agents designed for general use in targeting multiple epitopes are rare.

Here, we report the design, preparation, and characterization of new MR agents based on ordered and self-assembling DNA quadruplex scaffolds (19). The quadruplex-based DOTA (1,4,7,10-tetraazacyclododecane-1,4,7,10-tetraacetic acid) derivatives have almost 30-fold increased  $r_1$  versus clinical Gd-chelate contrast agents and two-fold increased  $r_1$  compared to the single oligonucleotide (ODN)-DOTA conjugate. These constructs further allow integration of bioactive functions to the quadruplex scaffolds leading potentially to the design of targeted contrast agents. Thus, these new agents provide a general template with high  $r_1$  molar relaxivity and ultrasmall size.

The ODN conjugated DOTAs were prepared by DNA solid phase coupling on a 1  $\mu\text{mol}$  scale. The 5'-ends of the quadruplex-forming oligonucleotides were tethered with DOTA (**1X** and **1Y**) (Figure 1). In **2X** and **2Y**, DOTA and DOTA dendrimers, respectively, were tethered to a single strand sequence that is incapable of forming self-assembled structures (Figure 1).

The synthesis of the modified oligonucleotides and the incorporation of Gd(III) ions (20) are detailed in the supporting information. Briefly, ODNs on the solid support were tethered with modifiers (5'-amino- modifier C6 were used to prepare **1X** and **2X**, while tribler phosphoramidite and 5'-amino-modifier 5 (see supporting information) were used to prepared **1Y** and **2Y**), which were then coupled with DOTA using Pybop and DIPEA in DMF overnight. The DOTA conjugated ODNs were subjected to deprotection in concentrated aqueous ammonia at 55 °C for 16 h, and incubated with gadolinium (III) citrate overnight at room temperature. The ODN conjugates were then purified by HPLC and confirmed by MALDI-TOF. Functionalized parallel quadruplexes were prepared in buffer (10 mM Tris-HCl, 80 mM KCl, pH 7.5) and incubated for 48 hr (21). The secondary structures of the complexes were confirmed by circular dichroism (CD) spectroscopy (Figure 2). The designed functionalized quadruplexes **1X** and **1Y** showed a positive ellipticity at 263 nm and a negative peak at 241 nm, which is characteristic of tetramolecular parallel quadruplex (22-24). In contrast,

incubation of **2X** and **2Y** only showed a weak signal at 273 nm and a negative peak at 250 nm in the CD spectrum, indicating no quadruplex formation.

The  $r_1$  of the contrast agents was measured by MRI with concentrations of samples confirmed by inductively coupled plasma (ICP)-MS measurements (see supporting data for methods). Compared to the single DNA-DOTA counterpart **2X**, the efficacy of the contrast agents have been highly improved through formation of the quadruplex. **1X** displays a relaxivity of  $11.7 \text{ mM}^{-1} \text{ s}^{-1}$  per Gd(III) ion and  $46.8 \text{ mM}^{-1} \text{ s}^{-1}$  per DNA quadruplex molecular complex, while **2X** has a relaxivity of  $6.4 \text{ mM}^{-1} \text{ s}^{-1}$  per Gd(III) and per molecule (Figure S1). The relaxivity of **2X** is in the normal range of currently used clinical contrast agents, yet, **1X** shows a two times increased relaxivity per Gd(III). This per complex  $r_1$  is higher than that of contrast agents based on a previously reported genetically engineered protein (11) and a reported synthetic dendrimer-based contrast agents ( $\sim 35 \text{ mM}^{-1} \text{ s}^{-1}$ ) (26). Importantly, this is the case even though our quadruplex-based agents have much lower molecular weight and the increase in  $r_1$  is likely due to the more ordered features of the DNA aggregate. Of note, the  $r_1$  of **1X** matches that of a recently reported, similarly sized (14 kDa) Gd-conjugated contrast agent (5). This agent is a Gd-conjugated to the C2A domain of synaptotagmin which is specific for phosphatidylserine (PS), whereas **1X** is designed for general use in targeting multiple epitopes.

The hypothesis that quadruplex formation increases the relaxivity of their contrast agents is further supported by studying a Gd-DOTA dendrimer conjugated DNA system. **1Y** displays a relaxivity of  $12.9 \text{ mM}^{-1} \text{ s}^{-1}$  per Gd(III) ion and  $154.8 \text{ mM}^{-1} \text{ s}^{-1}$  per DNA quadruplex complex, while **2Y** has a relaxivity of  $6.0 \text{ mM}^{-1} \text{ s}^{-1}$  per Gd(III) and per molecule (Figure S1). The relaxivities are comparable between **2X** to **2Y**, probably due to the flexibility of the linkers within the DOTA dendrimers. But again, **1Y** shows a two-fold increased relaxivity per Gd(III) compared to **2Y** and a much higher relaxivity per quadruplex than **1X**, since those Gd (III) ions are contained within each strand. We also observe a mode of increase in relaxivity per Gd(III) ion from **1X** to **1Y**, which is probably because formation of the ordered DNA quadruplex offsets the flexibility of the linkers within the dendrimer.

Other contrast agents conjugated to viruses, various proteins and Gd-conjugated synthetic polymers have been reported to display higher  $r_1$  values per molecule (27,28). However, the Gd-conjugated DNA quadruplex contrast agents reported here have several advantages including a low molecular weight and small size (2-3 nm), which could prove critical for targeted delivery and detection of specific cells or tissues, even behind intact blood vessels. Second, the DNA construct occurs naturally in the body and is biodegradable, potentially mitigating toxic effects. Third, the size of the quadruplex contrast agents can be easily modified by varying the lengths of the DNA sequences. Fourth, it may be possible to obtain quadruplex CAs with higher relaxivity if DOTA dendrimers with more rigid linkers can be tethered on the end of DNA quadruplex scaffold with shorter linker lengths. Lastly, functionalized DNA quadruplexes have been shown to target specific proteins (19,29), leaving open the possibilities of functionalizing the quadruplex with fragments that target specific cells or tissues.

In conclusion, we have described the design and synthesis of high-relaxivity DNA quadruplexes that can serve as improved MRI contrast agents. The ordered structure of the quadruplex leads to an increase in the relaxivities of the new MRI contrast agents. Further improvements in gadolinium relaxivity and packaging can be expected by conjugating Gd-DOTA dendrimers with rigid and short-length linkers as well as tethering bioactive groups to the DNA for use in targeted diagnosis.

## Supplementary Material

Refer to Web version on PubMed Central for supplementary material.

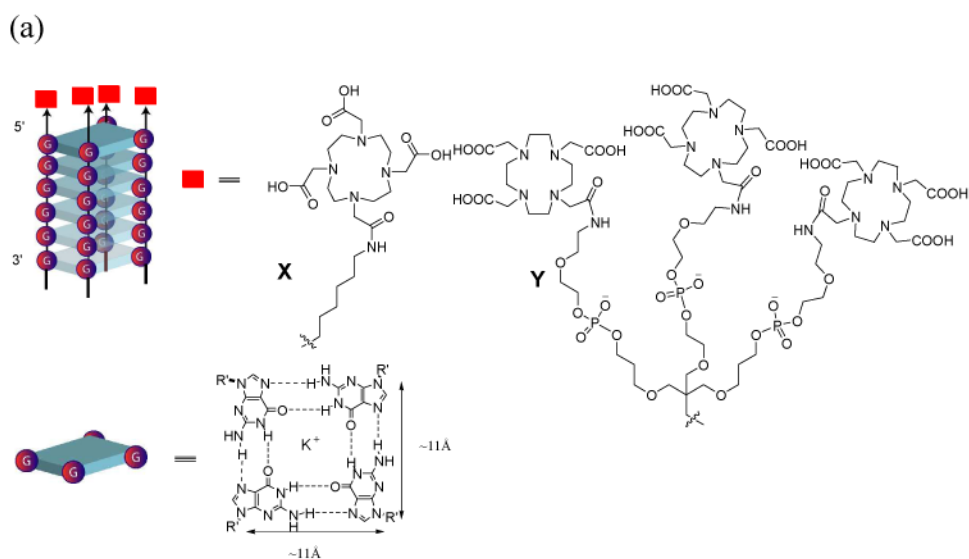
## Acknowledgements

We thank the National Institute of Health (NIH) (P30 NS-052519) and the National Science Foundation (NSF) (CHE-0750357) for financial support of this work.

## Literature Cited

1. Shapiro EM, Sharer K, Skrtic S, Koretsky AP. In vivo detection of single cells by MRI. *Magn Reson Med* 2006;55:242–9. [PubMed: 16416426]
2. Mulder WJ, Strijkers GJ, van Tilborg GA, Griffioen AW, Nicolay K. Lipid-based nanoparticles for contrast-enhanced MRI and molecular imaging. *NMR Biomed* 2006;19:142–64. [PubMed: 16450332]
3. Tran TD, Caruthers SD, Hughes M, Marsh JN, Cyrus T, Winter PM, Neubauer AM, Wickline SA, Lanza GM. Clinical applications of perfluorocarbon nanoparticles for molecular imaging and targeted therapeutics. *Int J Nanomedicine* 2007;2:515–26. [PubMed: 18203420]
4. Artemov D. Molecular magnetic resonance imaging with targeted contrast agents. *J Cell Biochem* 2003;90:518–24. [PubMed: 14523986]
5. Krishnan AS, Neves AA, de Backer MM, Hu DE, Davletov B, Kettunen MI, Brindle KM. Detection of cell death in tumors by using MR imaging and a gadolinium-based targeted contrast agent. *Radiology* 2008;246:854–62. [PubMed: 18187402]
6. Artemov D, Mori N, Ravi R, Bhujwalla ZM. Magnetic resonance molecular imaging of the HER-2/neu receptor. *Cancer Res* 2003;63:2723–7. [PubMed: 12782573]
7. Briley-Saebo KC, Mulder WJ, Mani V, Hyafil F, Amirbekian V, Aguinaldo JG, Fisher EA, Fayad ZA. Magnetic resonance imaging of vulnerable atherosclerotic plaques: current imaging strategies and molecular imaging probes. *J Magn Reson Imaging* 2007;26:460–79. [PubMed: 17729343]
8. Artemov D, Bhujwalla ZM, Bulte JW. Magnetic resonance imaging of cell surface receptors using targeted contrast agents. *Curr Pharm Biotechnol* 2004;5:485–94. [PubMed: 15579038]
9. Muldoon LL, Sandor M, Pinkston KE, Neuwelt EA. Imaging, distribution, and toxicity of superparamagnetic iron oxide magnetic resonance nanoparticles in the rat brain and intracerebral tumor. *Neurosurgery* 2005;57:785–96. [PubMed: 16239893]
10. Xie J, Chen K, Lee HY, Xu C, Hsu AR, Peng S, Chen X, Sun S. Ultrasmall c(RGDyK)-coated Fe<sub>3</sub>O<sub>4</sub> nanoparticles and their specific targeting to integrin  $\alpha(v)\beta_3$ -rich tumor cells. *J Am Chem Soc* 2008;130:7542–3. [PubMed: 18500805]
11. Karfeld LS, Bull SR, Davis NE, Meade TJ, Barron AE. Use of a Genetically Engineered Protein for the Design of a Multivalent MRI Contrast Agent. *Bioconjugate Chem* 2007;18:1697–1700.
12. Caravan P, Ellison JJ, McMurry TJ, Lauffer RB. Gadolinium(III) Chelates as MRI Contrast Agents: Structure, Dynamics, and Applications. *Chem Rev* 1999;99:2293–352. [PubMed: 11749483]
13. Langereis S, de Lussanet QG, van Genderen MH, Meijer EW, Beets-Tan RG, Griffioen AW, van Engelshoven JM, Backes WH. Evaluation of Gd(III)DTPA-terminated poly(propylene imine) dendrimers as contrast agents for MR imaging. *NMR Biomed* 2006;19:133–41. [PubMed: 16450331]
14. Bull SR, Guler MO, Bras RE, Meade TJ, Stupp SI. Self-Assembled Peptide Amphiphile Nanofibers Conjugated to MRI Contrast Agents. *Nano Lett* 2005;5:1–4. [PubMed: 15792402]
15. Gianolio, Eliana; G, GB.; Longo, Dario; Longo, Irene; Menegotto, Ivan; Aime, Silvio. Relaxometric and Modelling Studies of the Binding of a Lipophilic Gd-AAZTA Complex to Fatted and Defatted Human Serum Albumin. *Chemistry - A European Journal* 2007;13:5785–5797.
16. Yang JJ, Yang J, Wei L, Zurkiya O, Yang W, Li S, Zou J, Zhou Y, Maniccia ALW, Mao H, Zhao F, Malchow R, Zhao S, Johnson J, Hu X, Krogstad E, Liu ZR. Rational Design of Protein-Based MRI Contrast Agents. *J Am Chem Soc* 2008;130:9260–9267. [PubMed: 18576649]
17. Zhang, Zhaoda; G, MT.; Spiller, Marga; McMurry, Thomas J.; Lauffer, Randall B.; Caravan, Peter. Multilocus Binding Increases the Relaxivity of Protein-Bound MRI Contrast Agents. *Angew Chem Int Ed* 2005;44:6766–6769.
18. Sitharaman B, Kissell KR, Hartman KB, Tran LA, Baikalov A, Rusakova I, Sun Y, Khant HA, Ludtke SJ, Chiu W, Laus S, Toth E, Helm L, Merbach AE, Wilson LJ. Superparamagnetic gadonanotubes are high-performance MRI contrast agents. *Chemical Communications* 2005:3915–3917. [PubMed: 16075070]

19. Tagore DM, Sprinz KI, Fletcher S, Jayawickramarajah J, Hamilton AD. Protein recognition and denaturation by self-assembling fragments on a DNA quadruplex scaffold. *Angew Chem Int Ed Engl* 2007;46:223–5. [PubMed: 17136788]
20. Jaakkola L, Ylikoski A, Hovinen J. Solid-phase oligonucleotide labeling with DOTA. *Curr Protoc Nucleic Acid Chem* 2007;Chapter 14(Unit 4 31)
21. Jayawickramarajah J, Tagore DM, Tsou LK, Hamilton AD. Allosteric control of self-assembly: modulating the formation of guanine quadruplexes through orthogonal aromatic interactions. *Angew Chem Int Ed Engl* 2007;46:7583–6. [PubMed: 17823899]
22. Dapic V, Abdomerovic V, Marrington R, Peberdy J, Rodger A, Trent JO, Bates PJ. Biophysical and biological properties of quadruplex oligodeoxyribonucleotides. *Nucleic Acids Res* 2003;31:2097–107. [PubMed: 12682360]
23. Balagurumoorthy P, Brahmachari SK. Structure and stability of human telomeric sequence. *J Biol Chem* 1994;269:21858–69. [PubMed: 8063830]
24. Balagurumoorthy P, Brahmachari SK, Mohanty D, Bansal M, Sasisekharan V. Hairpin and parallel quartet structures for telomeric sequences. *Nucleic Acids Res* 1992;20:4061–7. [PubMed: 1508691]
25. Caravan P, Ellison JJ, McMurry TJ, Lauffer RB. Gadolinium(III) Chelates as MRI Contrast Agents: Structure, Dynamics, and Applications. *Chem Rev* 1999;99:2293–2352. [PubMed: 11749483]
26. Kobayashi H, Brechbiel MW. Dendrimer-based nanosized MRI contrast agents. *Curr Pharm Biotechnol* 2004;5:539–49. [PubMed: 15579043]
27. Aime, Silvio; F, L.; Crich, Simonetta Geninatti. Compartmentalization of a Gadolinium Complex in the Apoferritin Cavity: A Route To Obtain High Relaxivity Contrast Agents for Magnetic Resonance Imaging13. *Angew Chem Int Ed* 2002;41:1017–1019.
28. Allen M, Bulte JW, Liepold L, Basu G, Zywicke HA, Frank JA, Young M, Douglas T. Paramagnetic viral nanoparticles as potential high-relaxivity magnetic resonance contrast agents. *Magn Reson Med* 2005;54:807–12. [PubMed: 16155869]
29. Sprinz KI, Tagore DM, Hamilton AD. Self-assembly of bivalent protein-binding agents based on oligonucleotide-linked organic fragments. *Bioorg Med Chem Lett* 2005;15:3908–11. [PubMed: 15993069]



(b)

Oligonucleotide	Sequence
<b>1X</b>	[X-d(TGGGGGGTTTT)] <sub>4</sub>
<b>2X</b>	[X-d(CGTCATATCTTA)]
<b>1Y</b>	[Y-d(TGGGGGGTTTT)] <sub>4</sub>
<b>2Y</b>	[Y-d(TGTCATATCTTT)]

**Figure 1.**

(a) Functionalized parallel G-quadruplex with DOTA appendages. (b) Sequences of the designed oligonucleotides where G-quadruplex **1X** and **2Y** are tethered to DOTA or DOTA dendrimer fragments, respectively. **2X** and **2Y** are DOTA or DOTA dendrimer appended single strands that can not form quadruplex structure.

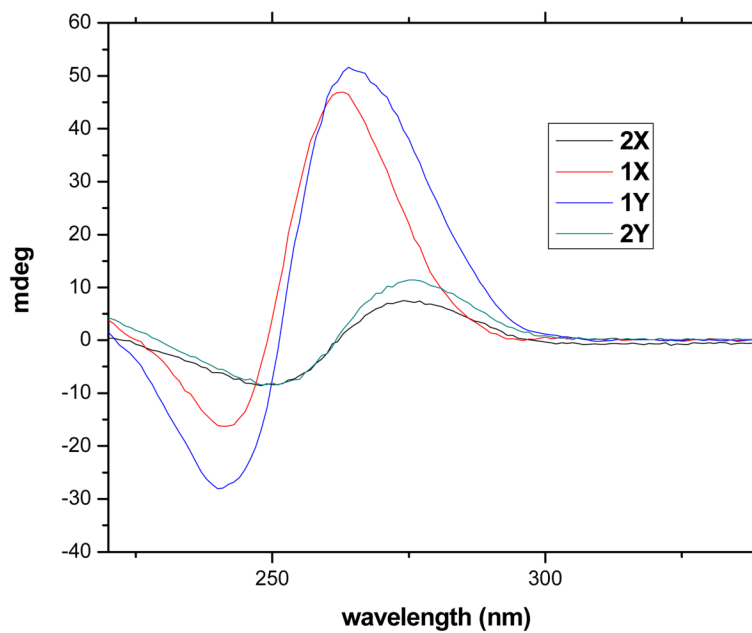


**Figure 2.** Circular dichroism spectra of ODNs after self-assembly. All measurements were done in 80 mM KCl, 10 mM Tris-HCl, pH 7.5 buffer. Concentrations of all ODNs were 60  $\mu$ M for the single strand.

**Table 1**

Gd(III) ionic and molecular relaxivities of standard MRI contrast agents and new agents **1X**, **2X**, **1Y** and **2Y** at 4.0 Tesla and 20.5 °C.

DNA	MW(g/mol) (based on DNA single strand)	Gd ionic $r_1$ ( $\text{mM}^{-1} \text{s}^{-1}$ )	no. of Gd	Molecular $r_1$ ( $\text{mM}^{-1} \text{s}^{-1}$ )
<b>1X</b>	4150.1	11.7	4	46.8
<b>2X</b>	4315.0	6.4	1	6.4
<b>1Y</b>	5920.9	12.9	12	154.8
<b>2Y</b>	6088.0	6.0	3	18
<b>GdDTPA</b> (8)	743	4.5	1	4.5
<b>GdDOTA</b> (25)	561	3.5	1	3.5